We are IntechOpen,
the world's leading publisher of
Open Access books
Built by scientists, for scientists

4,800
Open access books available

122,000
International authors and editors

135M
Downloads

Our authors are among the

154
Countries delivered to

TOP 1%
most cited scientists

12.2%
Contributors from top 500 universities

CLARIVATE ANALYTICS
BOOK CITATION INDEX
INDEXED

WEB OF SCIENCE™

Selection of our books indexed in the Book Citation Index
in Web of Science™ Core Collection (BKCI)

Interested in publishing with us?
Contact book.department@intechopen.com

Numbers displayed above are based on latest data collected.
For more information visit www.intechopen.com

Nanoscale Cu Wiring by Electrodeposition in Supercritical Carbon Dioxide Emulsified Electrolyte

Masato Sone, Tetsuya Shimizu, Nao Shinoda and Tso-Fu Mark Chang

Additional information is available at the end of the chapter

Abstract

Novel electrodeposition (ED) techniques utilizing supercritical carbon dioxide (scCO$_2$) emulsions (SCE) are introduced. ScCO$_2$ has low surface tension and high compatibility with hydrogen. Thus, this method is applied in fine Cu wiring to allow the complete filling of Cu into nanoscale confined space. The electrochemical reactions are carried out in emulsions composed of an aqueous electrolyte, scCO$_2$, and surfactants. Three aspects in fine Cu wiring will be introduced, which are the dissolution of the Cu seed layer in the SCE, the gap-filling capability of the ED-SCE, and the contamination in the plated Cu. At first, the dissolution of the Cu seed layer in the SCE was observed. In order to prevent the dissolution of the Cu seed layer, the addition of Cu particles into the SCE was found to be effective. The electrolyte containing the SCE and the Cu particles is named scCO$_2$ suspension (SCS). The gap-filling capability was evaluated using test element groups (TEGs) with patterns of vias with a diameter of 70 nm and an aspect ratio of 5. Many defects were observed in the vias filled using the conventional electrodeposition (CONV) method. On the other hand, defect-free fillings were obtained by the ED-SCS method. Because of the high-pressure environment needed to form the scCO$_2$, the reaction cells are usually batch-type high-pressure vessels. In order to improve the feasibility of the ED-SCS technique, a continuous-flow reaction system is also proposed and examined using a round-type large-area TEG with a diameter of 300 mm. Complete fillings were obtained for vias with a diameter of 60 nm and an aspect ratio of 5 on the large-area TEG. This result was in good agreement with that of the batch-type reaction system and demonstrated the successful application of the continuous-flow system with ED-SCS.

Keywords: Copper, electrodeposition, wiring, supercritical fluid, carbon dioxide, nano-structure

1. Introduction

1.1. Application of Cu electrodeposition into integrated circuit technology

The fabrication of materials with smaller dimensions and higher reliability has been the research interest because of the miniaturization of the devices used in the semiconductor industry. The Semiconductor Industry Association's International Technology Roadmap for Semiconductors predicts that half pitch of dynamic random access memory will become 15.9 nm in 2018 [1]. Cu electrodeposition is a key technology for the fabrication of interconnects used in microelectronic devices and related packaging technologies [2]. Especially for densification of the microelectronics, electrodeposition is often used in the fabrication of the three-dimensional structures [3]. On the other hand, voids and pinholes found in the Cu wiring of the integrated device can cause problems for the miniaturized device. Therefore, a process allowing defect-free deposition of Cu into the nanoscale space is needed.

Problems causing the formation of the voids and the pinholes can be the high surface tension of the aqueous electrolyte [4], the adsorption of H_2 bubbles on the cathode [5], the dissolution of the Cu seed layer [6], and the uneven current density distribution [7]. In order to inhibit the formation of the voids, a precise bottom-up filling of the vias is needed [8]. There are various studies on the bottom-up filling [9–13]. For example, additives such as accelerators and suppressors in copper–sulfate–sulfuric acid electrolyte are used for filling the vias to allow defect-free bottom-up filling [3]. However, the additives can cause problems such as impurity and grain refinement, which lead to high electric resistance because of the accumulation of impurity atoms in the grain boundary regions, and the grain boundary itself can also be a barrier for electrical conduction [14]. Moreover, Shimada et al. found that the resistivity of the polycrystalline Cu interconnects increases with a decrease in the line width [15]. Therefore, a process allowing defect-free Cu wiring, reduction in usage of the additives, and decreasing numbers of the grain boundary is required.

1.2. Damascene process and the problems in nanosized miniaturization

Electrodeposition is one of the wiring formation methods used in the semiconductor production technology, especially in the formation of Cu wiring, namely, damascene Cu process [1,16]. In the damascene process, vias and trenches are made on a Si wafer, and Cu is filled into these vias by electrodeposition. The deposited Cu can diffuse into the Si wafers, so a barrier layer, such as TaN, is deposited first after making the vias and trenches on the Si wafer. In addition, a Cu layer is sputtered on top of the barrier layer as the seed layer in order to conduct the electrodeposition.

The filling of the vias by Cu electrodeposition technology has been realized from the development of electrochemical additives and so on [9–18]. However, a new technology is required for the demand of next-generation devices. For the miniaturization of interconnects in the devices, investigation on improvement of the dry processes, such as CVD and PVD [19,20], and electrodeposition methods [21] have been conducted. However, there are still many problems needed to be solved before the wiring technology can be practically used in the industries.

In order to solve these problems, electrodeposition using organic additives with varies functions has been proposed [10]. An example of the additives would be having bis(3-sulfopropyl disulfide) (SPS) as the accelerator and polyethylene glycol (PEG) as the suppressor with small amounts of Cl⁻. However, there are two problems in the filling of Cu using these additives. One is the impurity problem, which has been reported to cause high electric resistance problem in the electrodeposited Cu when large amounts of the additives are used [22]. The other is the dense grain boundary, which inhibits electron movement as that in the polycrystalline [15]. The dense grain boundary is caused by the accelerated nucleation and inhibited nuclei growth by the additives. Therefore, a novel method is needed to reduce amount of the additives used.

Metal deposition using supercritical fluid has received great attention recently [23–25]. Watkins et al. reported that the filling of Cu into vias having diameter below 100 nm can be achieved using supercritical CO_2 (scCO$_2$) [23, 24]. The complete filling of Cu into the vias arose from low surface tension and high solubility of H_2 in scCO$_2$ because scCO$_2$ is nonpolar and has properties between those of liquids and gases. However, also because of the nonpolar property, the solubility of metal salts is extremely low in scCO$_2$, and metal organic compounds are used to ensure enough metal ion concentration to conduct the electrodeposition. Then the organic by-products form during the reduction reaction become the source of impurity in the deposited metallic film.
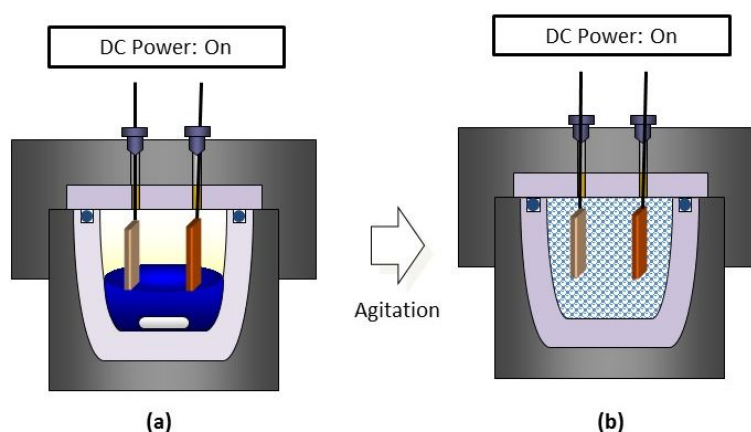

Figure 1. Schematic illustration of ED-SCS; (a) biphasic state before agitation and (b) electrodeposition in scCO$_2$ suspension.

1.3. Electrodeposition in supercritical carbon dioxide emulsions (ED-SCE)

We have proposed an electrodeposition method with supercritical carbon dioxide (scCO$_2$) emulsions [26–28], which was named ED-SCE, as shown in Fig. 1, to reduce the formation of defects in the electrodeposited materials. Supercritical fluids have properties between those of a gas and a liquid. Basically, the physical properties can be adjusted by controlling the temperature and pressure [29]. Among the commonly used solvents as the supercritical fluid, scCO$_2$ has received the most attention because of its relatively low critical points, which are

7.39 MPa and 304.25 K. In addition, CO_2 is nontoxic and abundant. However, electrodeposition cannot be conducted in pure CO_2 because both electrical conductivity and solubility of metal salts are low in CO_2. Therefore, surfactants were used to form emulsions composed of the aqueous electrolyte and $scCO_2$. Ni films fabricated by the ED-SCE were reported to be defect free because of the enhancement in removal of adsorbed H_2 gas bubbles on the surface of the cathode in the SCE [9]. The mechanism is expected to take place in the reduction reaction of Cu and reduce usage of the additives in fine Cu wiring process. In this chapter, experimental results on the application of the ED-SCE in the filling of Cu into nanoscale vias will be introduced. Moreover, an electrodeposition method in $scCO_2$ suspension (ED-SCS) is proposed for nanoscale Cu wiring for integrated circuit. Also, in order to apply the ED-SCS in nanoscale wiring of large-area via TEG, such as Si wafers with 300 mm diameter, a reaction apparatus of continuous-flow reaction system using the SCS is developed.

2. Cu electrodeposition using suspension of supercritical carbon dioxide in copper–sulfate-based electrolyte with Cu particles

2.1. Cu electrodeposition in supercritical carbon dioxide emulsions (ED-SCE)

2.1.1. The dispersion states of SCE

In a previous study, dispersion states of the SCE with Ni electrolyte (Watts bath) were observed through a high-pressure view cell [26]. In the case of Cu plating, it is essential to check the dispersion state of the SCE with the Cu electrolyte because viscosity and density of the Cu electrolyte are different from those of the Ni electrolyte. Fig. 2 shows the dispersion state of the SCE with the Cu electrolyte [30]. Without agitation, the electrolyte and $scCO_2$ were completely separated. After the agitation started, foams appeared near the interface between the gas and the electrolyte, and then the SCE was formed. The outlook of the SCE with the Cu electrolyte was similar with that of the Ni electrolyte, although the colors were different from each other. Thus, the SCE with the Cu electrolyte is clearly applicable for the ED-SCE.
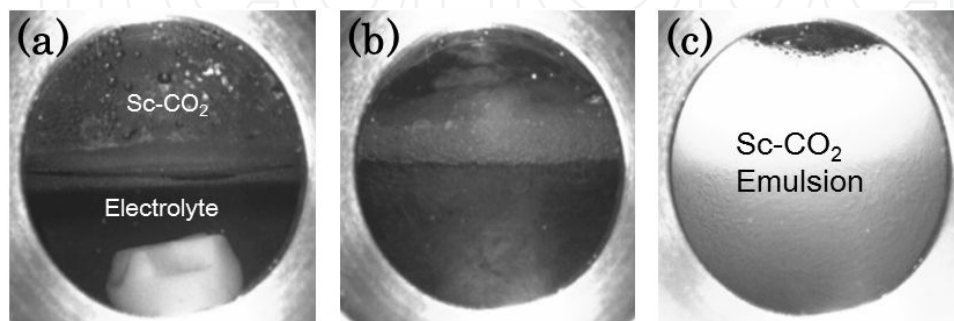

Figure 2. The dispersion state of SCE through view cell: (a) two separated phase of $scCO_2$ and the electrolyte, (b) immediately after stirring, and (c) SCE.

2.1.2. Dissolution of the Cu seed layer on TEG in SCE

The high-pressure experimental apparatus is shown in Fig. 3. Temperature variation of each run was confirmed to be less than 1.0 K. Maximum working temperature and maximum pressure were 424 K and 50 MPa, respectively. The reaction chamber was a stainless steel 316 vessel with a volume of 50 ml and lined with polyether ether ketone (PEEK) coating. The high-pressure vessel was placed in a box oven for control of the temperature. There were holes at the chamber cap for inflow and outflow of CO_2 and connection of the electrodes. Through the holes, platinum wires inserted in PEEK tube were used to position the substrates and connected to a programmable power supply. A magnetic agitator with a cross-shaped magnetic stirrer bar was placed in the reaction chamber for mixing.
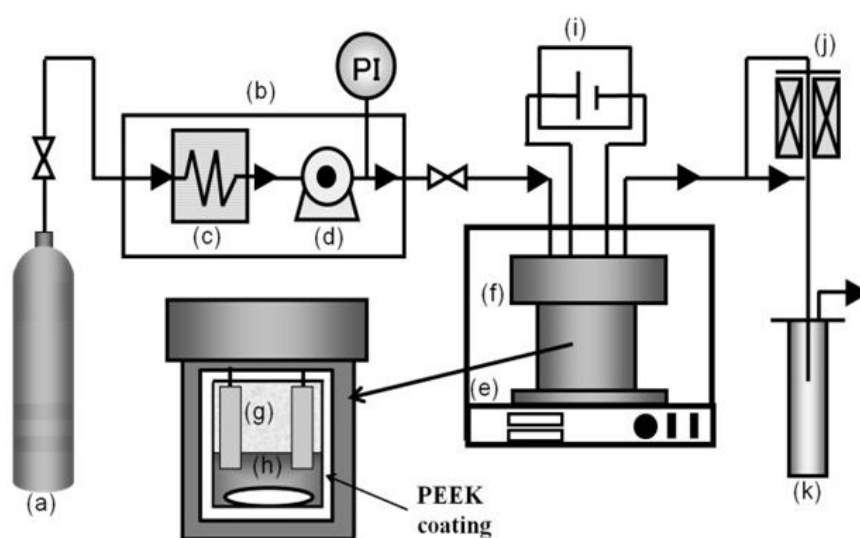

Figure 3. Experimental apparatus; (a) CO_2 gas tank, (b) CO_2 liquidization unit, (c) liquidization unit, (d) high-pressure pump, (e) thermal bath, (f) reaction cell (SUS316L) with PEEK coating inside, (g) substrate, (h) cross stirrer, (i) power supply, (j) back pressure regulator, and (k) trap.

Fig. 4(a) shows an optical microscope (OM) image of the TEG before the electrode position reaction, and the color of the surface was like the color of Cu because the top layer was the Cu seed layer. Fig. 4(b) shows the surface of the TEG after the ED-SCE for 10 min. The color of Cu could not be observed in Fig. 4(b), which indicated the disappearance of the Cu seed layer on the TEG after the ED-SCE for 10 min, and the grey color should be from the color of the TaN barrier layer. In fact, Martyak and Ricou reported damage of the Cu seed layer after immersion in a sulfuric acid-based electrolyte [17]. The dissolution of the Cu seed layer in the ED-SCE is suggested to be caused by the carbonic acid formed after the dissociation of CO_2 into the electrolyte. The formation of the carbonic acid leads to an increase in H^+ concentration in the electrolyte and a decrease in pH. In this way, Cu dissolution would be accelerated in the SCE with the sulfuric acid-based Cu electrolyte. In order to inhibit the dissolution of the Cu seed layer, the Cu electrodeposition was conducted in the SCS formed by the addition of Cu particles into the SCE, and the result is shown in Fig. 4(c). The seed layer was intact, and Cu was successfully electrodeposited on the TEG.
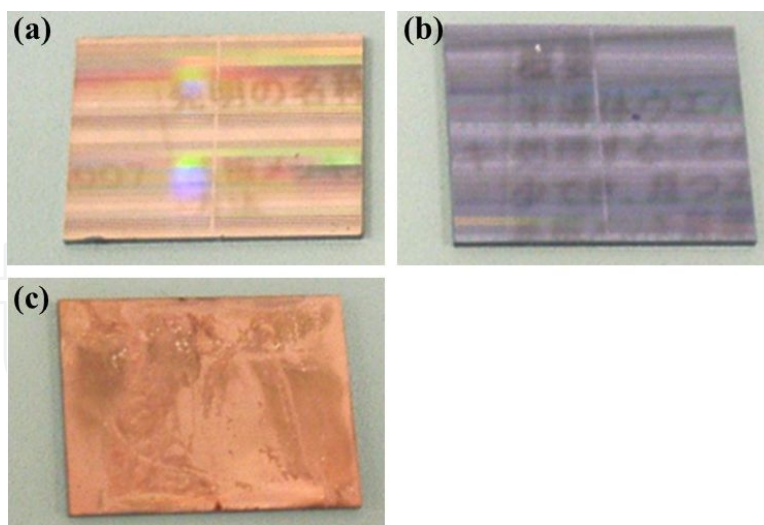
Figure 4. OM images of the TEG (a) before the electrodeposition reaction, (b) after ED-SCE for 10 min, and (c) after ED-SCS for 10 min.

2.1.3. Comparison of current efficiency between emulsions of scCO₂ and hexane

Physical properties of hexane are similar to those of $scCO_2$; hence, hexane is used to confirm effects of $scCO_2$ in the ED-SCE [27]. Cu plate (99.99 mass%) with dimensions of 2.0×1.0 cm^2 was used as the working electrode to evaluate surface morphology of the electrodeposited Cu films and measurement of the current efficiency (CE). Pt plate with the same dimensions was used as the counter electrode. The CE was calculated using Equation (1), where the weight difference before and after 1 h of deposition time is used, as follows:

$$CE = \frac{\text{Final Weight-Initial Weight}}{\text{Weight of Cu deposted at 100\% CE}} \times 100\% \qquad (1)$$

Fig. 5 shows the CE as a function of the volume fraction of the dispersed phase. The base electrolyte used here was additive-free sulfuric acid-based electrolyte [31,32]. The CE without the dispersed phase indicates that only the base electrolyte was used. The CE was found to decrease with an increase in the volume fraction of the $scCO_2$. In a previous study, this loss of CE was considered to be caused by the evolution of H_2 or increased electrical resistance after increasing the volume fraction of the nonelectrical conductive content, such as CO_2 [27]. The CEs in $scCO_2$ emulsions are all lower than those in the hexane emulsions. This phenomenon was not reported in a previous study on the ED-SCE of Ni [27]. The decrease in the CEs was suggested to be caused by the dissolution of Cu in the SCE.

2.1.4. Dissolution of Cu in scCO₂ emulsions

In this section, the dissolution of Cu in the ED-SCE is discussed. Fig. 3 shows weight loss of the Cu plate immersed in different acidic electrolytes with different immersion times. Weights
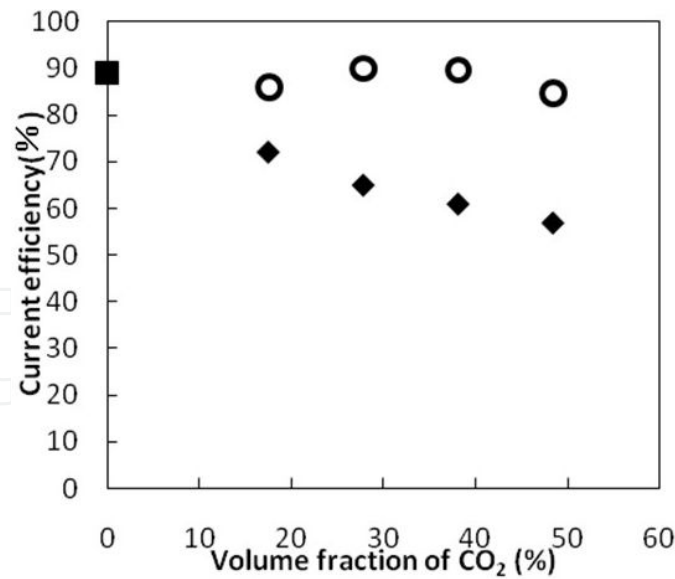
Figure 5. Current efficiency as a function of CO_2 volume fractions in hexane emulsions and $scCO_2$ emulsions additive-free base electrolyte at 1.0 A/dm² and 1 h deposition time (■:base electrolyte; ○: hexane emulsions; ◆: $scCO_2$ emulsions).

of the Cu loss after immersion in all of the copper–sulfate-based electrolytes for 2 hours were compared. In the conventional electrolyte, 1.25 mg/cm² of Cu was dissolved. In the SCE, 0.55 mg /cm² of Cu was dissolved. The results showed that the dissolution of Cu was accelerated in the SCE. The dissociation of CO_2 into the electrolyte can cause an increase in acidity of the solution and lead to a higher dissolution rate of the Cu seed layer. Thus, the ED-SCE is not appropriate for the Cu damascene process.

The acidic electrolytes are the base electrolyte with pH 3.2, the SCE using the pH 3.2 base electrolyte, and the base electrolyte with pH adjusted to 3.0 by the addition of H_2SO_4. Weights of Cu loss were found to increase with an increase in the immersion time in all of the electrolytes. These results show that the copper–sulfate-based electrolyte can also cause the dissolution of Cu. Cho et al. suggested that the dissolution of Cu and CuO in sulfuric acid-based-solution would occur by the following chemical reactions [6]:

$$CuO + 2H^+ \rightleftharpoons Cu^{2+} + H_2O \qquad (2)$$

$$2Cu + O_2 + 4H^+ \rightleftharpoons 2Cu^{2+} + 2H_2O \qquad (3)$$

$$Cu + 2Cl^- \longrightarrow CuCl_2^- + e^- \qquad (4)$$

However, in this study, Equations (2) and (4) could not occur because oxides were removed in the pretreatment steps, and Cl⁻ was not added at this point. In this case, the dissolution of

Cu should be caused by Equation (3). On the other hand, Fig. 3 shows dissolution rate of Cu was higher in the SCE when compared with the pH 3.2 base electrolyte. We believe this was caused by the dissociation of CO_2 in the electrolyte as shown in the following reactions [33].

$$CO_2 + H_2O \rightleftharpoons H_2CO_3 \tag{5}$$

$$H_2CO_3 \rightleftharpoons H^+ + HCO_3^- \tag{6}$$

$$HCO_3^- \rightleftharpoons H^+ + CO_3^{2-} \tag{7}$$

These reactions led to an increase in H^+ concentration in the electrolyte, and the pH was decreased. The low pH and O_2 dissolved in the electrolyte could accelerate the dissolution of Cu according to Equation (3). The weight of Cu lost in the pH 3.0 base electrolyte shown in Fig. 6 was approximately the same as that in the SCE, which indicated that the pH of the SCE might be close to 3.0.
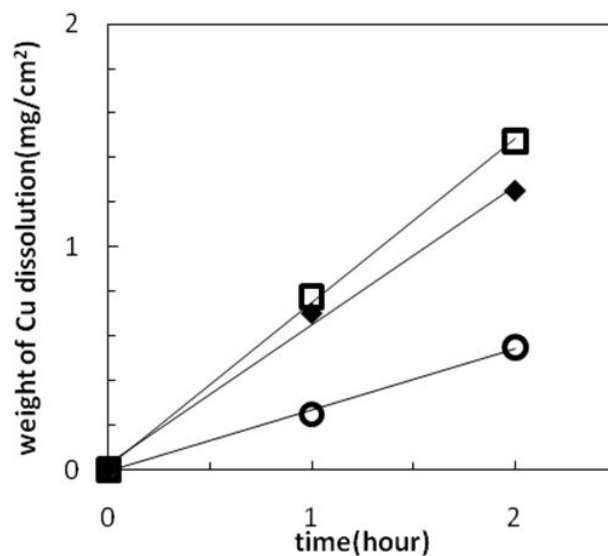

Figure 6. Weight loss of Cu substrate when immersed in different solutions with different immersion time. (○: pH 3.2 base electrolyte; ◆:scCO$_2$ emulsions using pH 3.2 base electrolyte; □: pH 3.0 base electrolyte).

2.2. Cu electrodeposition in supercritical carbon dioxide suspension (ED-SCS)

2.2.1. Current efficiency of ED-SCS and comparison between amount of additives needed in CONV and ED-SCS

In order to inhibit the dissolution of the Cu seed layer, Cu electrodeposition in scCO$_2$ suspension denoted as ED-SCS was conducted. The dissolution of the seed layer is expected to be low when the concentration of the Cu ions in the electrolyte is saturated. Therefore, CuSO$_4$ particles were added to the electrolyte forming a suspension to maintain the Cu ion concentration at

the saturation level. However, the dissolution was still observed. Then 1.7 g/L of pure Cu particles was used to form the suspension, and the CE was increased when comparing with the cases without the Cu particles. In addition, the CE was almost the same as that of the CONV, as shown in Fig. 7.
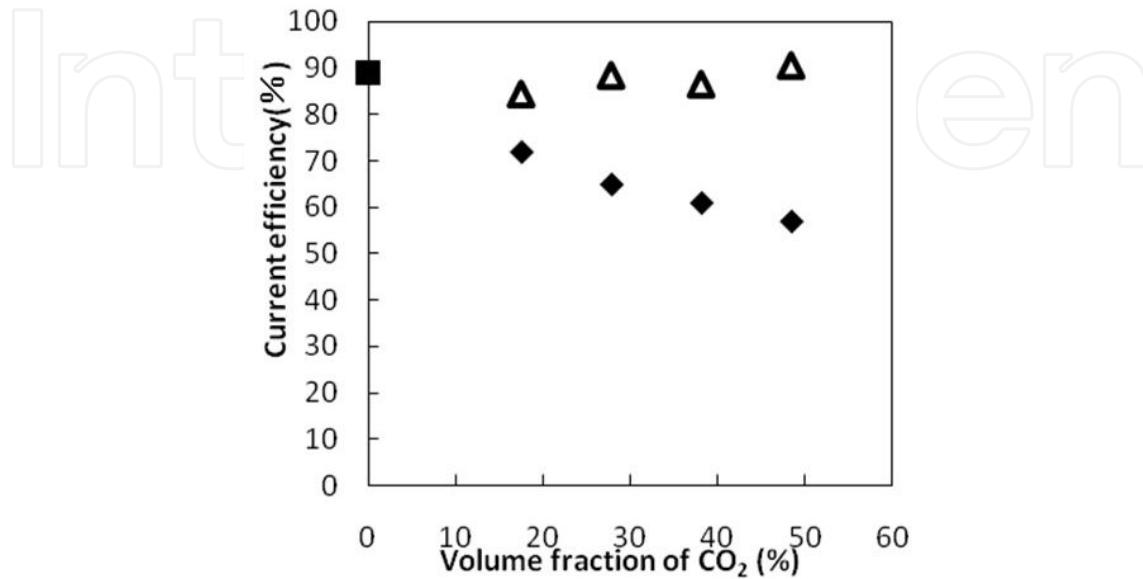

Figure 7. Current efficiency of CONV, ED-SCE, and ED-SCS with Cu particles (1.7 g/L) using additive-free base electrolyte at 1.0 A/dm^2 and 1 h deposition time (■: CONV; ◆:ED-SCE; △: ED-SCS).

2.2.2. Application of ED-SCS in the filling of nanoscale vias

Next, filling capability was evaluated using the TEG having vias with a diameter of 70 nm and an aspect ratio of 2 by the CONV and the ED-SCS, as shown in Fig. 8. In Fig. 8(a), the vias were filled by the CONV, but there were many defects. The Cu electrolyte is a commercially available electrolyte designed to fill vias with an aspect ratio of 1 only, and this result supported the ability of the Cu electrolyte to fill nanoscale vias. The formation of the voids can be caused by (1) the dissolution of the Cu seed layer, (2) the high surface tension of the electrodeposition solution to cause difficulties in transferring the electrolytes to bottom of the vias, (3) the evolution of H_2 to hinder the Cu deposition, or (4) the conformal crystal growth mechanism caused by the current distribution. The result shows that the dissolution of the Cu seed layer did not occur; thus, voids were caused by Equation (2), (3), or (4). On the other hand, Cu can be filled into the vias with no voids and pinholes by the ED-SCS as shown in Fig. 8(b). Thus, the ED-SCS is more effective for filling Cu into nanoscale vias when comparing with the CONV.

Moreover, we applied the ED-SCS in the filling of vias with a diameter of 70 nm and an aspect ratio of 5, as shown in Fig. 9(a). For the ED-SCS, the complete filling of all the vias with electrodeposited Cu was observed with no void, as shown in Fig. 9(c). These complete gap-filling results by the ED-SCS demonstrated that the SCS was effective in improving transport
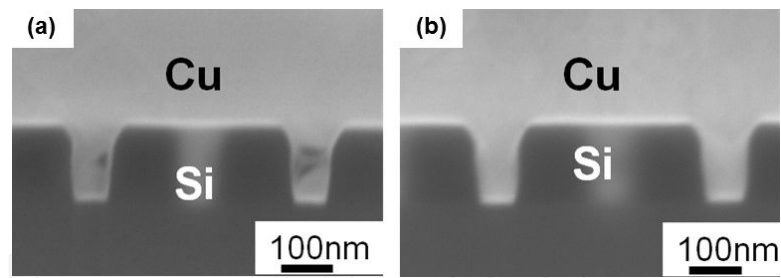
Figure 8. Cross-sectional SEM images of via test element group (TEG) with vias with a diameter of 70 nm and an aspect ratio of 5 filled (a) by conventional electrodeposition of Cu and (c) by ED-SCS of Cu.

properties of the electrolyte and minimizing problems caused by the generation of H_2 bubbles. In addition, the ED-SCS might have the ability to fill recessed features with the bottom-up or super-conformal growth mechanisms, which can be utilized to completely fill the recessed parts [11,34–37]. However, more study is required to know the detailed filling mechanism.
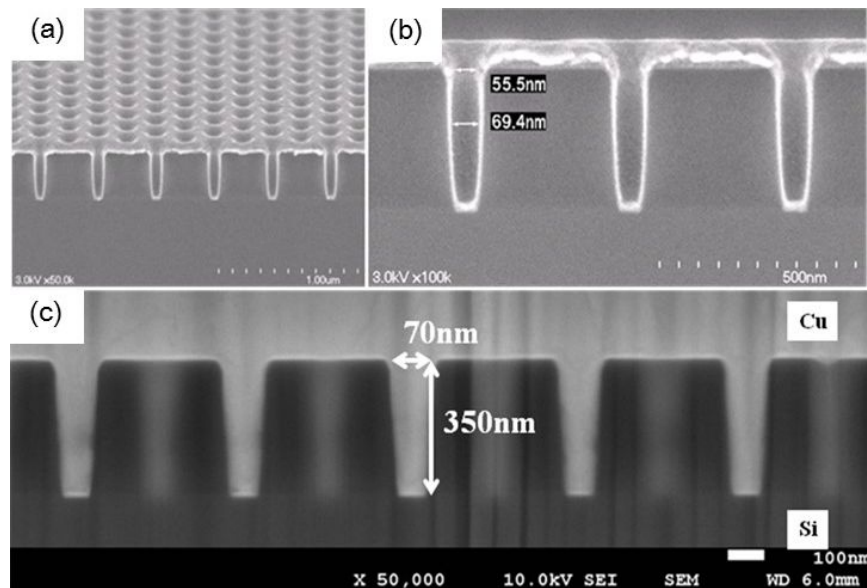

Figure 9. Cross-sectional SEM images of (a) Via test element group (TEG) with vias with a diameter of 70 nm and an aspect ratio of 5, (b) expanded image of (a), and (c) TEG filled with Cu electrodeposited in scCO$_2$ suspension.

2.2.3. Crystal structure of the electrodeposited Cu filled inside the vias by ED-SCS

Fig. 10 shows a cross-sectional TEM image of electrodeposited Cu filled into the TEG with a diameter of 60 nm and an aspect ratio of 2 by the ED-SCS. All of the vias were filled by the electrodeposited Cu without any voids. Moreover, it is interesting that the electrodeposited Cu filled into the two vias at the bottom left of Fig. 10 are both single crystals, and the electrodeposited Cu inside the two vias from the upper right shows few twin boundaries parallel to the bottom surface of the TEG. These twin boundaries in the electrodeposited Cu were confirmed to be Cu crystal along [111] crystallographic orientation by dark-field image and

bright-field image of TEM [30]. Studies have shown that void-free and complete filling of Cu into nanoscaled vias are usually caused by the bottom-up growth and the conformal growth mechanisms, and the conformal growth is not suitable for the filling of Cu into nanosized vias by electrodeposition [8]. However, if conformal growth occurred in the ED-SCS reaction system, columnar grain could be formed along center line of the vias because Cu crystal would grow from inner walls of the vias. Nevertheless, of the few twin boundaries parallel to the bottom surface observed, the crystal growth mechanism in the ED-SCS is suggested to be the bottom-up growth mechanism.
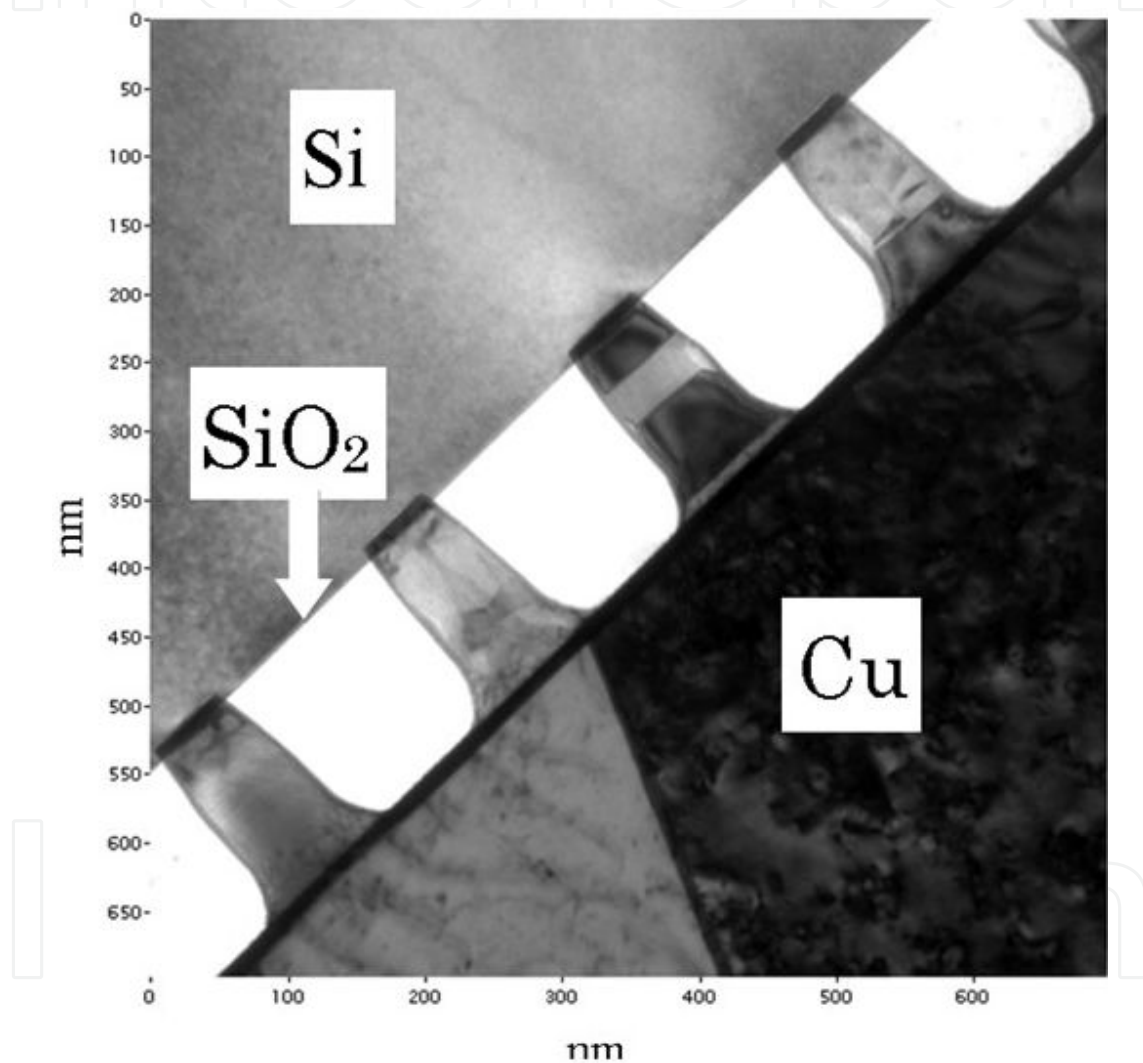

Figure 10. Cross-sectional TEM image of Cu filled by ED-SCS into via TEG with a diameter of 60 nm and an aspect ratio of 2.

2.3. Contamination in electrodeposited Cu

Ni films obtained by the ED-SCE were found to contain carbon content higher than the Ni films obtained by the conventional electrodeposition methods [38,39]. Carbon impurities

would cause the high electric resistance problem in electrodeposited Cu [40]. Thus, it is necessary to investigate the concentration of impurity(s) in the Cu films obtained by the ED-SCS. The impurity could be carbons, organics, and/or oxides. Thus, the concentration of carbon and oxygen in the electrodeposited Cu films prepared by the ED-SCS was examined by glow discharge optical emission spectroscopy (GDOES) [41]. Fig. 11(a) shows that the carbon concentration profile in the Cu film fabricated by the conventional electrodeposition method was very close to that of the Cu film fabricated by the ED-SCS. These results indicated that, unlike the case of Ni ED-SCE, the level of carbon impurity in the Cu film is about the same between the ED-SCS and the conventional electrodeposition method.
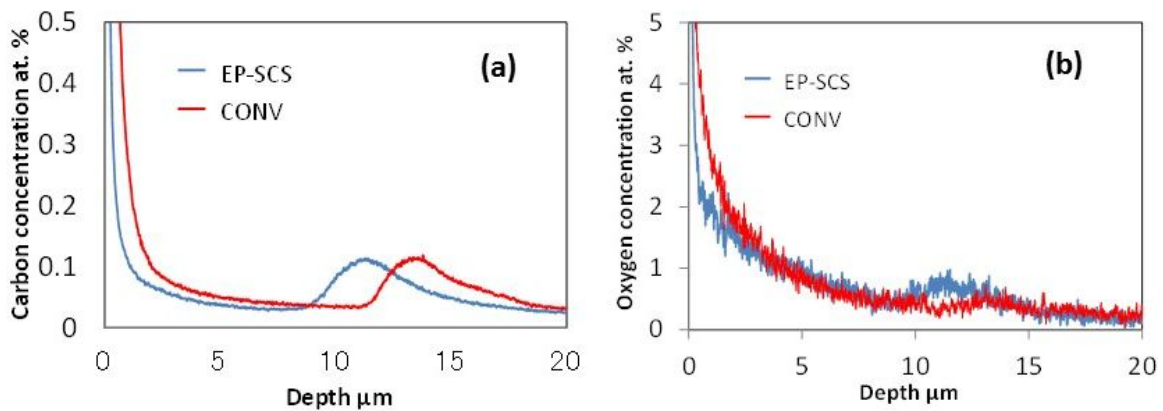

Figure 11. Glow discharge optical emission spectra of (a) carbon and (b) oxygen content in the electrodeposited Cu by conventional method (CONV) and ED-SCS.

In this reaction, a nonionic surfactant $C_{12}H_{25}(OCH_2CH_2)_{15}OH$ was added into the electrolyte for the formation of the $scCO_2$ suspension in the ED-SCS. Therefore, the influence of the surfactant in the electrodeposited Cu films in terms of impurity should be evaluated. The influence of the surfactant was investigated by measuring the concentration of oxygen content in the films. Fig. 11(b) shows the oxygen concentration profile in the Cu film fabricated by the conventional electrodeposition method and the ED-SCS. Again, the oxygen content in the two Cu films was about the same. Therefore, the results confirmed that the surfactant used in this system would not cause further impurity problem in the electrodeposited films.

2.4. Summary

In this section, electrodeposition in the $scCO_2$ suspension to fill nanoscale vias with high aspect ratio and prevent the formation of void and pinhole by using a Cu electrolyte originally designed to fill vias with an aspect ratio of 1 was evaluated. Complete and defect-free fillings were obtained even when the aspect ratio was increased to 5. This indicated that the amount of the additives used can be significantly decreased by the ED-SCS. In addition, the electrical conductivity of Cu filled into the nanovia is expected to be better because of the less grain boundary formed in Cu filled by the ED-SCS.

3. Cu wiring into nanoscale vias by ED-SCS with a continuous-flow reaction system

3.1. Application of ED-SCS into nanoscale wiring with large-area via TEG

In the previous section, the electrodeposition method using SCS (ED-SCS) has been proved to be effective in allowing the complete filling of Cu into nanoscale vias [30–32]. The vias were 70 nm in diameter with an aspect ratio of 5, and the electrolyte used was a commercial available copper sulfate-based electrolyte design to fill vias with aspect ratio of 1. However, the reaction cell used was a batch-type reactor with small dimensions, which limit the practical application of the ED-SCS in the industries. A system capable of processing substrates with large diameter is required, and it will be even better to have a continuous-flow-type reaction system.

In order to apply ED-SCS into nanoscale wiring with large-area via TEG, the homogenization of the SCS in the high-pressure reaction chamber becomes critical. Mechanical agitation used in the batch-type system is not sufficient to ensure the homogenization of the SCS because of the density difference between the $scCO_2$, the electrolyte, and the Cu particles [27]. Therefore, a continuous-flow reaction system for the ED-SCS is developed to solve the problems mentioned. One of the advantages for a continuous-flow reaction system involving supercritical fluid is that additional depressurization step is not required for the exchange of the processed substrate and the electrolytes [42,43]. In addition, economically, energy and production efficiency of a continuous-flow reaction system are usually better than those of a batch-type reaction system.

For the continuous-flow reaction system, a round-type via TEG with a diameter of 300 mm is used to demonstrate advantages and feasibility of the system. In addition, the nanoscale vias on the TEG would have a diameter of 60 nm with aspect ratios of 2 and 5.

3.2. Design of the continuous-flow reaction apparatus and reaction procedures

Fig. 12 shows the continuous-flow reaction system. Line A goes through the reaction chamber to conduct the electrochemical reactions, and line B is used only for mixing to allow the homogenization of the SCS. The total inner volume of the continuous-flow reaction system without line B is 15.5 L. The inner volume of line A is the same as line B. This reaction system is composed of a reaction chamber having a volume of 1.82 L, a storage chamber for the aqueous electrolyte with a volume of 3.1 K, and a canned pump (RW99-216C2L-0204S1V-B, Teikoku Electric MFG. CO., Ltd) with maximum flow rate of 50 L/min. All units are connected by stainless steel (SUS-316) pipes with 3/4 inch diameter. The inner wall of the pipes are lined with gold to provide corrosion resistance against the SCS. Temperatures in this system are measured at 6 points denoted as (T#), and pressures are also measured at 2 points denoted as (P#) in the process flow diagram (Fig. 12). Switching of the flow between lines A and B can be done on the digital control panel.

Details of the reaction chamber are shown in Fig. 13. The cathode and the anode are located at the top and bottom of the chamber with a distance of 20 mm in between. The via TEG is attached to the cathode, and the anode is a piece of gold plate. The SCS is injected into the reaction
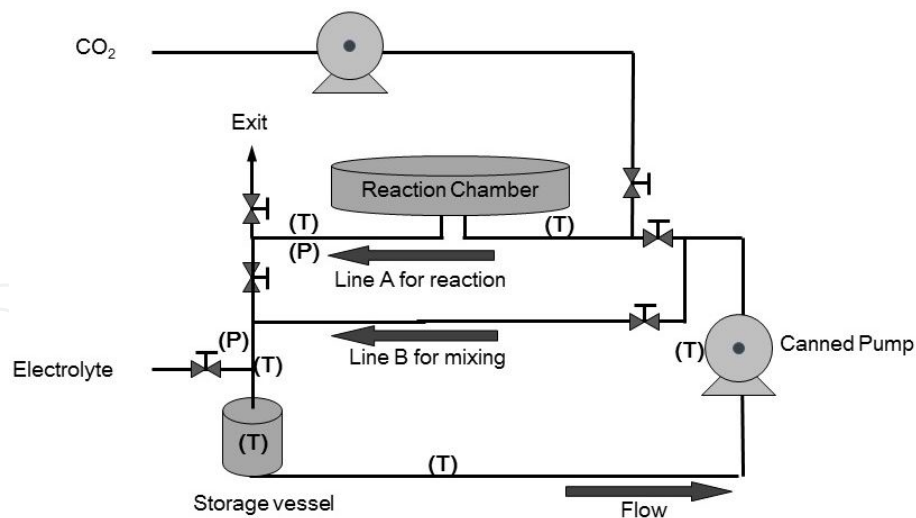
Figure 12. Experimental apparatus of the continuous-flow reaction system. This reaction system is composed of a reaction chamber, a storage vessel for the aqueous electrolyte, and a canned pump. T and P indicate the points to measure temperature and pressure in system, respectively.

chamber through four entrees (3/4 inch diameter SUS316 tube) and is excreted from the outlet (3/4 inch diameter) located at the middle of the reaction chamber, as shown in Fig. 13.
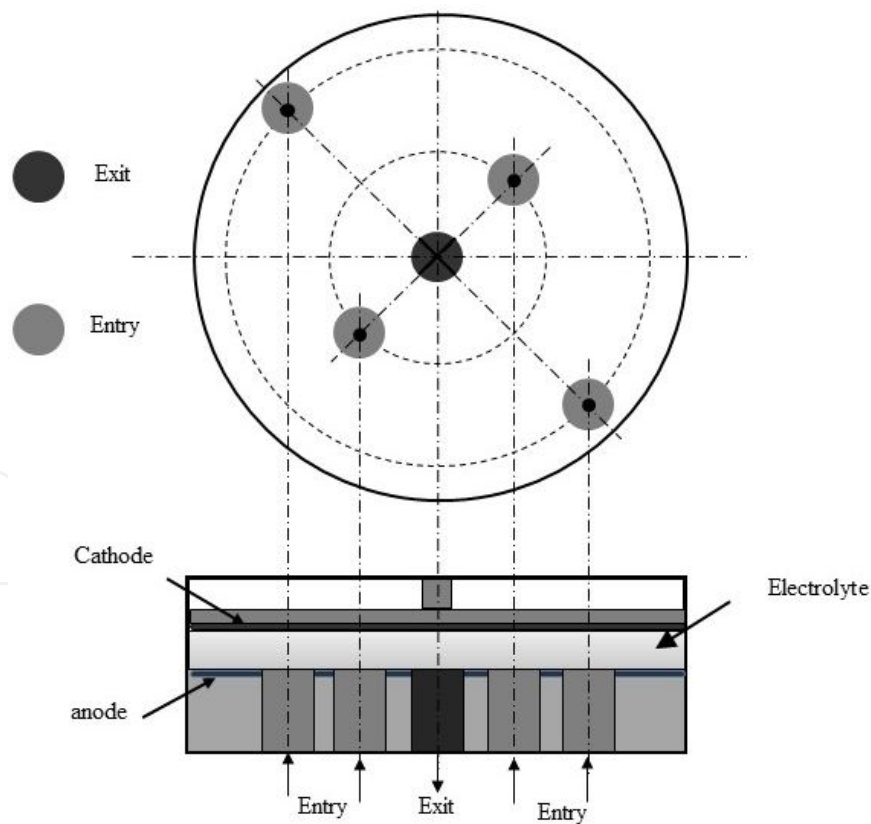

Figure 13. Detailed structure of the reaction chamber. Upper illustration shows positions of entrees and outlet for circulating the $scCO_2$ suspension. Lower illustration is a cross-sectional image of the reaction chamber and shows geometry of electrodes, four entrees, and outlet. The diameter of reaction area is 300 mm, and distance between cathode and anode is 20 mm.

In this system, the reaction steps were described in the following steps. First, 12 L of the aqueous Cu electrolyte with the surfactant and Cu particles were injected into line B of the system by a pump, which indicates that the Cu electrolyte would occupy 77.4% of volume in the system. Second, pressurized CO_2 was introduced into the system through a liquidization unit (composed of a compressor and a high-pressure pump), and the pressure was maintained at the desired value. Third, the temperature was raised to the desired value. Fourth, Cu electrolyte, surfactants, Cu particles, and $scCO_2$ were mixed by circulating the flow in the continuous-flow system at a flow rate of 25 L/min via line B for 10 min to homogenize the emulsions or the suspension. This step was also necessary to ensure Cu ion concentration in the SCS reached the saturation concentration to prevent the dissolution of the Cu seed layer on the TEG. Fifth, the SCS was introduced to the reaction chamber through line A of the continuous-flow system, and then the ED-SCS reaction was conducted for 10 min. Finally, the flow was changed back to line B, and the pressure and electrolyte left in line A and reaction chamber would be excluded. Then the via TEG with electrodeposited Cu could be obtained.
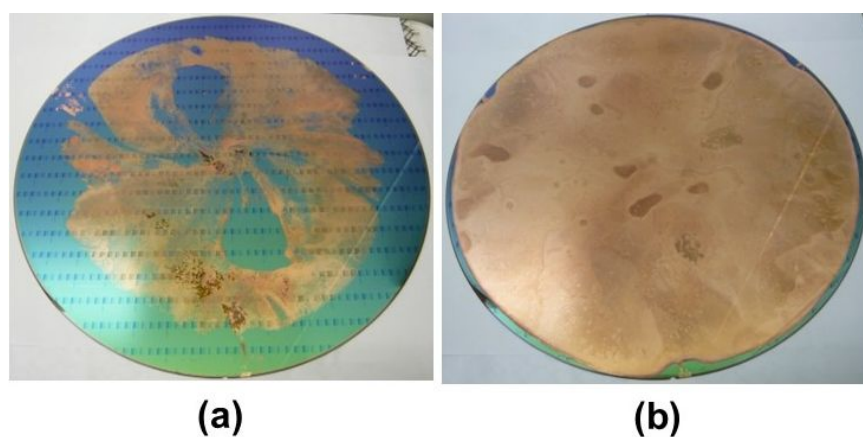

Figure 14. Photographic images of the 300-mm diameter round-type via TEG after ED-SCS. The applied currents are (a) 1.41 A/dm² and (b) 2.83 A/dm².

3.3. Cu electrodeposition on large-scale TEG

The SCS was composed of a commercially available copper sulfate-based electrolyte, pure Cu particles, CO_2, and a surfactant [$C_{12}H_{25}(OCH_2CH_2)_{15}OH$, as reported in the previous section. The additives used were 1.0×10^{-4} mol/L of polyethylene glycol with molecular weight of 8000 g/mol, 2.94×10^{-5} mol/L of Janus green B, 2.1×10^{-5} mol/L of bis(3-sulfopropyl) disulfide, and 1.7×10^{-3} mol/L of Cl⁻ (NaCl). Regarding the reaction conditions, 23 vol.% of CO_2 at 313 K and 12 MPa were used. Three values of direct current were used, that is, 10, 20, and 30 A, which correspond to current density values of 1.41, 2.83, and 4.23 A/dm², respectively. TEGs with a diameter of 300 mm and cylindrical-shaped vias with (I) 60 nm diameter and 120 nm depth and (II) 60 nm diameter and 300 nm depth were fabricated on the Si wafers, where Cu seed layer (12~13 nm thick on the inner wall and 50~60 nm thick on the top surface)/TaN barrier layer (3~4 nm thick on the inner wall and 15 nm on the top surface) was deposited on the Si wafer by sputtering. The anode was a gold-electrodeposited Cu plate with a diameter of 300 mm.

The surface of the electrodeposited Cu film on the TEG was observed by a digital camera (Sony Cyber-shot DSC-WX5). As shown in Fig. 14(a), the surface of the TEG was not completely covered with electrodeposited Cu when the current density was 1.41 A/dm^2. The diameter and the depth of the vias on the TEGs shown in Fig. 14 were 60 nm and 120 nm, respectively. However, the surface of the TEG was completely covered with bright Cu film by the ED-SCS when the current density was 2.83 A/dm^2, as shown in Fig. 14(b). This result was unexpected because a current density of 1.41 A/dm^2 with the batch system was enough for the complete coverage of the TEG surface with electrodeposited Cu and also for the filling of the nanovias, reported in previous studies [30–32]. The mechanism causing this phenomenon is still not clarified yet. It is suggested that the flow speed can also affect nucleation rate of Cu on the substrate, and the flow speed used in a continuous-flow reaction system is much higher than the flow caused by a mechanical agitation system in a batch-type reaction system. Therefore, a current density of 1.41 A/dm^2 was not enough to have complete coverage of the TEG surface and filling of the vias when the continuous-flow reaction system was used. A more detailed investigation on the effects of the flow patterns on the electrodeposition of Cu with the continuous-flow reaction system will be conducted and reported in the future.
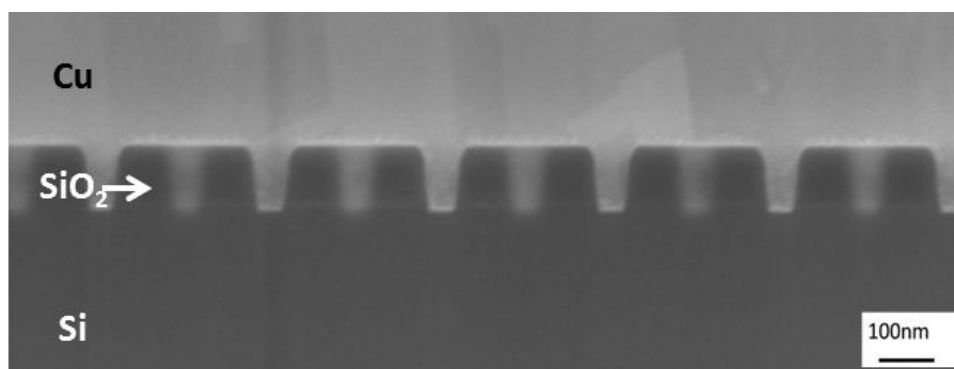

Figure 15. Cross-sectional SEM images of Cu filled into nanoscale vias (60 nm diameter, 120 nm depth) by ED-SCS with the continuous-flow reaction system with current density 2.83 A/dm^2 of applied direct current.

3.4. Wiring into nanoscale via

Cross-sectional images of the vias filled with the electrodeposited Cu were observed by a scanning electron microscope (SEM). Cross section of the TEG (the one shown in Fig. 14(b)) with vias of 60 nm in diameter and 120 nm in depth was observed by SEM, as shown in Fig. 15. The current density used here was 2.83 A/dm^2. The complete filling of the electrodeposited Cu in all of the vias was observed with no voids. These complete gap-filling results were achieved because the transfer of the reactive species into the nanoscale confined space is improved by the scCO$_2$ to fill such fine vias with high aspect ratio, and the addition of the Cu particles in the SCE suppressed the dissolution of the Cu seed layer. This result was in good agreement with that of the batch-type reaction system [31] and demonstrated the successful application of the continuous-flow system with the ED-SCS.
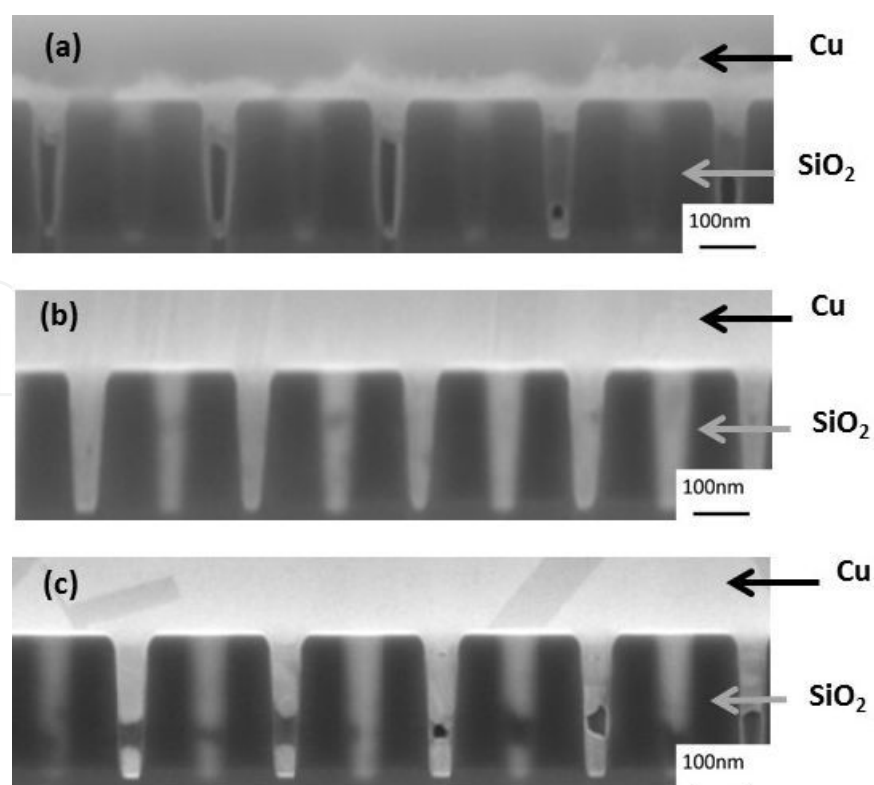
Figure 16. Cross-sectional SEM images of Cu filled in nanoscale vias (60 nm diameter, 300 nm depth) by ED-SCS with the continuous-flow reaction system; (a) 1.41 A/dm^2), (b) 2.83 A/dm^2, and (c) 4.23 A/dm^2 of applied direct current.

The filling capability of the ED-SCS was confirmed to be further improved with the continuous-flow reaction system when comparing with the batch-type reaction system. Fig. 16 shows the filling of the electrodeposited Cu into the nanoscale vias with 60 nm diameter and 300 nm depth by the ED-SCS with the continuous-flow reaction system as a function of direct current, where a diameter of the vias used in this study was smaller than the vias used in the previous study for the batch-type reaction system [32]. The complete filling of all the vias with 60 nm diameter and 300 nm depth was observed when the current density was 2.83 A/dm^2 (Fig. 16(b)). This result indicated that the gap-filling capability of the ED-SCS is higher with this continuous-flow reaction system than the batch-type reaction system, where the vias with 60 nm diameter and 300 nm depth could not be completely filled by the batch-type reaction system. The result demonstrated that the homogeneity of the suspension was better in the continuous-flow system, which allows the improvement in the filling ability.

On the other hand, results of the filling between the current density of 1.41 and 4.23 A/dm^2 were completely different. Incomplete filling, that is, only the opening section of the vias was filled with Cu, was observed in the nanoscale vias when 1.41 A/dm^2 was used, and the surface of the TEG was again not completely covered by the electrodeposited Cu. Voids at the middle section of the vias were observed when 4.23 A/dm^2 was used, while 4.23 A/dm^2 was enough to have the electrodeposited Cu completely covering the surface of the TEG. The incomplete filling for the 1.41-A/dm^2 case is believed to be mainly caused by insufficient overpotential to drive the Cu reduction reaction. For the filling of nanovias by electrodeposition, additives like

accelerators, suppressors, and inhibitors have to be used. Complete filling is obtained when the suppressors worked near the opening of the vias to prevent closing of the vias before complete filling is obtained, and the effect of the accelerator should be high at the bottom of the vias to allow the bottom-up growth mechanism to take place. In general, accelerators are more competitive for adsorption onto the surface, and suppressors are more competitive in terms of readsorption [44]. In this case, when the continuous-flow reaction system was used, the transport of materials would be improved, and hence readsorption of the suppressors used in this study and the suppressor effect would be enhanced [12]. Because of this, the suppressor effect would be too strong, and a higher cathodic overpotential would be required to initiate the Cu reduction reaction. According to the Butler–Volmer equation, low current density leads to low cathodic overpotential. When 1.41 A/dm^2 was used, the cathodic overpotential might be too low to initiate the reduction reaction of Cu. Therefore, both top surface and most of the space inside the vias were not covered or filled with the electrodeposited Cu. For the case of 4.23 A/dm^2, the voids observed in the vias were found to be located at middle of the vias. This indicated that the formation of the voids was caused by closing of the via opening before complete filling was achieved. In the other words, the current applied was too high to give a high cathodic overpotential. The high cathodic overpotential could cause desorption of the additives [45], especially the suppressors, and cause diminishing of the suppressor effects near the opening of the vias.

3.5. Summary

In order to apply the ED-SCS into nanoscale wiring with large-area TEGs patterned with nanoscale vias, a high-pressure reaction apparatus of continuous-flow reaction system using supercritical carbon dioxide was developed. Moreover, the filling capability was confirmed to be high for nanoscale vias having 60 nm in diameter and aspect ratios of 2 and 5 on the round-type large-area TEGs. The surface of the round-type via TEG was completely coated by the bright Cu, and all of the vias were completely filled by Cu without any defects using this system. Moreover, an impurity analysis confirmed that the ED-SCS would not cause any impurity problem in the electrodeposited Cu.

4. Conclusions

In this paper, Cu electrodeposition processes were conducted in the scCO$_2$ suspension. The dissolution of the Cu seed layer in the ED-SCE was observed and believed to be caused by the low pH caused by the formation of the carbonic acid from the dissociation of CO$_2$ into the aqueous electrolyte. In addition, the current efficiency of the ED-SCE decreased with an increase in the CO$_2$ volume fraction. Thus, the ED-SCS was applied to inhibit the dissolution of the Cu seed layer and to improve the current efficiency. Cu films obtained by the ED-SCS were smooth and bright film without any pinholes, and the usage of the additives can be reduced significantly. Moreover, we applied the ED-SCS technique with a reduced amount of additives in filling the nanoscale vias with high aspect ratio. The Cu electrolyte used was a commercially available electrolyte originally designed to fill vias with an aspect ratio of 1.

When the ED-SCS was applied, void-free and complete filling was achieved because of the low surface tension and viscosity of the $scCO_2$ and suppression of the Cu seed layer dissolution. Also, the application of the $scCO_2$ suspension as the electrolyte of Cu wiring showed a possibility to decrease the amount of the additives used because the gap-filling capability of the ED-SCS was better than the conventional method. Moreover, an impurity analysis, GDOES, confirmed that the ED-SCS would not cause any impurity problem in the electrodeposited Cu. In order to apply the ED-SCS into nanoscale wiring with large-area via TEG, such as round silicon wafers with 300 mm diameter, a reaction apparatus of continuous-flow reaction system using supercritical carbon dioxide was developed. The filling capability of Cu into nanoscale vias with 60 nm diameter and aspect ratios of 2 and 5 on the round-type via TEG was evaluated. The surface of the round-type via TEG was completely coated uniformly by bright Cu, and all of the vias were completely filled by Cu without any defects using this system.

Acknowledgements

Author details

Masato Sone[*], Tetsuya Shimizu, Nao Shinoda and Tso-Fu Mark Chang

*Address all correspondence to: sone.m.aa@m.titech.ac.jp

Precision and Intelligence Laboratory, Tokyo Institute of Technology, Nagatsuta-cho Midori-ku, Yokohama, Japan

References

[1] Semiconductor Industry Association, 2011 International Technology Roadmap for Semiconductor (Semiconductor Industry Association, Incheon, Korea, 2011).

[2] M. Gad-el-Hak, The MEMS Handbook (CRC, Taylor & Francis, Boca Raton, Florida, 2006).

[3] O. Luhn, A. Radisic, C.V. Hoof, W. Ruythooren, J.P. Celis, *J. Electrochem. Soc.*, 157 (2010) D242.

[4] B.C. Baker, C. Witt, D. Josell, T.P. Moffat, *Electrochem. Solid-State Lett.*, 6 (2003) C67.

[5]   W.L. Tsai, P.C. Hsu, Y. Hwu, C.H. Chen, L.W. Chang, J.H. Je, M.H. Lin, A. Groso, G. Margaritondo, *Nature*, 417 (2002) 139.

[6]   S.K. Cho, T. Lim, H.K. Lee, J.J. Kim, *J. Electrochem. Soc.*, 157 (2010) D187.

[7]   De Virgiliis, O. Azzaroni, R.C. Salvarezza, E.V. Albano, *Appl. Phys. Lett.*, 82 (2003) 1953.

[8]   T.P. Moffat, L.Y. Ou Yang, *J. Electrochem. Soc.*, 157 (2010) D228.

[9]   T.P. Moffat, D. Wheeler, W.H. Huber, D. Josell, *Electrochem. Solid State Lett.*, 4 (2001) C26.

[10] D. Josell, D. Wheeler, T.P. Moffat, *J. Electrochem. Soc.*, 5(2002) C49.

[11] T.P. Moffat, J.E. Bonevich, W.H. Huber, A. Stanishevsky, D.R. Kelly, G.R. Stafford, D. Josell, *J. Electrochem. Soc.*, 147 (2000) 4524.

[12] S.M. Huang, C.W. Liu, W.P. Dow, *J. Electrochem. Soc.*, 159 (2012) D135.

[13] W.P. Dow, M.Y. Yen, C.W. Liu, C.C. Huang, *Electrochim. Acta*, 53 (2008) 3610.

[14] J.D. Budai, C.W. White, S.P. Withrow, M.F. Chisholm, J. Zhu, R.A. Zuhr. *Nature*, 390 (1997) 384.

[15] M. Shimada, M. Moriyama, K. Ito, S. Tsukimoto, M. Murakami, *J. Vac. Sci. Technol.*, B24(2006) 190.

[16] C. Andricacos, C. Uzoh, J.U. Dukovic, J. Horkans, H. Deligiani, *IBM J. Res. Dev.*42 (1998) 567.

[17] L.T. Koh, G.Z. You, S.Y. Lim, C.Y. Lim, P.D. Foo, *Microelectron.J.*32 (2001) 973.

[18] M. Tan, J.N. Harb, *J. Electrochem. Soc.*, 150 (2003) C420.

[19] T. Momose, M. Sugiyama, Y. Shimogaki, *J. Appl. Phys.*44 (2005) L1199.

[20] E. Kondoh, J. Fukuda, *J. Supercrit. Fluids*, 44 (2008) 466.

[21] N. Tantavichet, M.D. Pritzker, *J. Electrochem. Soc.*, 150 (2003) C665.

[22] M. Stangl, M. Liprak, J. Acker, V. Hoffman, S. Baunack, K. Wetzig, *Thin Solid Films*, 517 (2009) 2687.

[23] J.M. Blackburn, D.P. Long, A. Cabanas, J.J. Watkins, *Science*, 294(2001) 141.

[24] Y. Zong, J.J. Watkins, *Chem. Mater.*, 17 (2005) 560.

[25] E. Kondoh, K. Shigama, *Thin Solid Films*, 491(2005) 228.

[26] H. Yoshida, M. Sone, H. Wakabayashi, H. Yan, K. Abe, X.T. Tao, A. Mizushima, S. Ichihara, S. Miyata, *Thin Solid Films*, 446(2004) 194.

[27] H. Yan, M. Sone, N. Sato, S. Ichihara, S. Miyata, *Surf. Coat. Technol.*, 182 (2004) 329.

[28] T.M. Chang, M. Sone, A. Shibata, C. Ishiyama, Y. Higo, *Electrochem. Acta*, 55 (2010) 6469.

[29] T. Clifford, Fundamentals of Supercritical Fluids (Oxford University Press, United Kingdom, 1999).

[30] T. Shimizu, N. Shinoda, T.F.M. Chang, A. Shibata, M. Sone, *Surf. Coat. Technol.*, 231 (2013) 77.

[31] N. Shinoda, T. Shimizu, T.F.M. Chang, A. Shibata, M. Sone, *Thin Solid Films*, 529 (2013) 385.

[32] N. Shinoda, T. Shimizu, T.F.M. Chang, A. Shibata, M. Sone, *Microelectro. Eng.*, 97 (2012) 126.

[33] N.M. Martyak, P. Ricou, *Mater. Sci. Semicond. Process.*, 6 (2003) 225.

[34] E.D. Niemeyer, F.V. Bright, *J. Phys. Chem.*, 102 (1998) 1474.

[35] Hovestad, L. Janssen, *Modern Aspects of Electrochemistry*, 38 (2005) 475.

[36] K. Pantleon, J.A.D. Jensen, M.A.J. Somers, *J. Electrochem. Soc.*, 151 (2004) C45.

[37] J. Reid, *J. Appl. Phys.*, 40(2001) 2650.

[38] S.T. Chung, W.T. Tsai, *J. Electrochem. Soc.*, 156 (2009) D457.

[39] T. Nagoshi, T.F.M. Chang, T. Sato, M. Sone, *Microelectr. Eng.*, 110 (2013) 269.

[40] T. Osaka, N. Yamachika, M. Yoshino, M. Hasegawa, Y. Negishi, Y. Okinaka, *Electrochem. Solid State. Lett.*, 12 (2009) D15.

[41] T. Shimizu, T.F.M. Chang, Y. Ishimoto, H. Kinashi, T. Nagoshi, T. Sato, M. Sone, *J. Supercrit. Fluids*, 90 (2014) 60.

[42] H. Machida, M. Takesue, R.L. Smith Jr., *J. Supercrit. Fluids*, 60 (2011) 2.

[43] J.R. Hyde, P. Licence, D. Carter, M. Poliakoff, *Appl. Catal. A,* 222 (2001) 119.

[44] P. Broekmann, A. Fluegel, C. Emnet, M. Arnold, C. Roeger-Goepfert, A. Wagner, N.T.M. Hai, D. Mayer, *Electrochim. Acta*, 56 (2011) 4724.

[45] J.G. Long, P.C. Searson, P.M. Vereecken, J. Electrochem. Soc., 153 (2006) C258.